



Ultraviolet photolysis of metformin: mechanisms of environmental factors, identification of intermediates, and density functional theory calculations

Wenting Lin¹ · Xiaohan Zhang¹ · Ping Li¹ · Yongzhen Tan¹ · Yuan Ren^{1,2,3}

Received: 1 October 2019 / Accepted: 26 February 2020 / Published online: 7 March 2020
© Springer-Verlag GmbH Germany, part of Springer Nature 2020

Abstract

As a commonly used anti-diabetic drug, metformin (MEF) is frequently detected in different water bodies which pose a potential threat to human health and the ecological environment. In this study, oxidative degradation of MEF under ultraviolet (UV) light was studied, and its influencing factors, photolysis mechanism, and intermediates identification carried out as well. The results showed that the hydroxyl radical contributed 73% during the 6 h MEF photolysis process among the reactive oxygen species (ROS). In addition, triplet excited-state organic matter and singlet oxygen also played a role in the photolysis process. The reaction rates of hydroxyl radical and singlet oxygen with MEF are $(6.45 \pm 0.4) \times 10^9$ and $(5.4 \pm 0.7) \times 10^6 \text{ L} \cdot (\text{mol s})^{-1}$, respectively. By calculating the light screening effect of environmental factors, it is found that the presence of NO_3^- and Cl^- had a greater excitation effect on ROS than the screening effect, and generally promoted the photolysis rates of MEF from 90.3 to 193.5% and from 16.1 to 80.6% during the 6-h reaction process, respectively. For bicarbonate and fulvic acid, the light screening effects were dominant and inhibited photolysis rates by 10–52% and 13–71%, respectively. The results demonstrated that the photoreactivity of environmental factors in water is the cause of the different photodegradation rates of MEF. The oxidative degradation product of MEF under UV light was detected by UPLC/Q-TOF as methylbiguanide (MBG), 2,4-diamino-1,3,5-triazine (2,4-DAT), biguanide (BGN), 1,1-dimethylguanidine (1,1-DiMBG), 4-amino-2-imino-1-methyl-1,2-dihydro-1, 3,5-triazine (4,2,1-AIMT), and 2-amino-4-methylamino-1,3,5-triazine (2,4-AMT). The result which showed that the primary sites of ·OH attacked is consistent with that of density functional theory calculation.

Keywords Metformin · UV photolysis · Hydroxyl radicals · Light screening effect · Density functional theory · UPLC/Q-TOF

Responsible editor: Suresh Pillai

Electronic supplementary material The online version of this article (<https://doi.org/10.1007/s11356-020-08255-9>) contains supplementary material, which is available to authorized users.

✉ Yuan Ren
ceyren@scut.edu.cn

¹ School of Environment and Energy, South China University of Technology, Higher Education Mega Center, Panyu District, Guangzhou 510006, People's Republic of China

² The Key Lab of Pollution Control and Ecosystem Restoration in Industry Clusters, Ministry of Education, Guangzhou, People's Republic of China

³ The Key Laboratory of Environmental Protection and Eco-Remediation of Guangdong Regular Higher Education Institutions, Guangzhou, People's Republic of China

Introduction

According to a statistics in 2015, about 415 million people in the world aged 20–79 had diabetes (prevalence rate 8.8%), and 318 million people had impaired glucose tolerance (previous disease rate 6.7%) (Ogurtsova et al. 2017). If there is no intervention, according to the International Diabetes Federation (IDF), the number of global diabetes patients will reach 642 million in 2040, the pre-diabetes population will be 481 million, and the number of patients in China will rise to 154 million (Ogurtsova et al. 2017). At present, diabetes medication ranks second only to cancer medication in global drug sales (China Industry Information Network 2018). Diabetes is divided into types 1 and 2, of which type 2 diabetes accounts for approximately 90% of all cases. Metformin (MEF) is the basic drug for type 2 diabetes and its production in China in 2015 and 2016 was 4589 and 5039 T (Editorial Department of Annual Report 2018; Editorial Department of Annual Report

2017), respectively, the largest production volume among all anti-diabetic drugs.

After being taken by human body, 77% of MEF is discharged as a prototype compound to wastewater treatment plants (WWTPs) through sewage pipelines and finally discharged into the environment (Scheurer et al. 2012). At present, biodegradation and adsorption are the main measures of MEF removal in sewage treatment plants. It has been reported that the adsorption removal efficiency of activated sludge containing MEF was 20% (Tisler and Zwiener 2019) and its removal efficiency in sewage treatment plants was between 41 and 98% (Blair et al. 2015). It has been reported that the median MEF concentration was $110 \mu\text{g L}^{-1}$ in the influent of a German wastewater treatment plant and $11.4 \mu\text{g L}^{-1}$ in the effluent (Scheurer et al. 2009). Campbell measured the mineralization efficiency of MEF in an anaerobic sludge digester for 60 days as 82% and its half-life was 26 days (Campbell 2013). Trautwein et al. also found that MEF was degraded by approximately 50% in natural waters within 14 days (Trautwein and Kümmerer 2011). Residual MEF adversely affects aquatic organisms when discharged into natural waters. For example, it was reported that exposure of minnows to domestic wastewater containing MEF ($40 \mu\text{g L}^{-1}$) for 40 days had an adverse effect on their reproductive development and a greater negative impact on juvenile fish than adult fish (Crago et al. 2016; Niemuth and Klaper 2015). MEF is not a hormonal compound in structure, nor can it affect estrogen's physiological activities (Escher et al. 2011); however, studies have found that it can be used as an effective endocrine disorder drug to treat polycystic ovary syndrome (Tang et al. 2012). Therefore, MEF may be a potential, non-traditional endocrine disruptor in the environment and its ecological impact in water environments should be of concern along with its removal technology.

Compared with the ecotoxicological effects brought about by chlorine and ozone, ultraviolet (UV) disinfection is characterized by high efficiency, safety, and low cost, and is often used for the degradation of pharmaceuticals and personal care products (PPCPs) in water (Cheng et al. 2018; Ma et al. 2016). Photoexcited PPCPs can not only undergo direct photolysis in water but self-sensitized photolysis as well. Direct photolysis is a process in which pollutants can selectively absorb photons and directly decompose to form products. During this process, excited contaminants can also absorb photons to generate singlet or triplet excited-state reactive organic material ($^1\text{ROM}^*$ or $^3\text{ROM}^*$) to form products, or transfer energy to other compounds to form reactive oxygen species (ROS), such as singlet oxygen ($^1\text{O}_2$) and hydroxyl radical ($\cdot\text{OH}$), and, then, pollutant molecules will be further oxidatively degraded by these ROS (Yong et al. 2009). This is the so-called self-sensitized photolysis (Li et al. 2017). At present, there are few studies on the

photolysis of MEF under UV light, and these studies are mainly concentrated in pure water (Collin et al. 2004; Quintao et al. 2016), and there is no research, to the best of our knowledge, on the mechanisms and effect of other environmental factors on UV photolysis. In this study, as a target pollutant, MEF was used to investigate its oxidative degradation mechanism under UV light, and a density functional theory (DFT) calculation was first applied to predict the active sites of MEF reaction. The photolysis pathway is proposed according to the products identified by the UPLC/Q-TOF method. The results of this study provide a comprehensive understanding of the UV oxidation degradation process and its products of MEF in water environments, laying the foundation for assessing its impact on an ecosystem.

Materials and methods

Chemicals

MEF (>99.5%), methanol, acetonitrile, and ammonium acetate were HPLC-grade and purchased from ANPEL Laboratory Technologies, Inc. (Shanghai, China). Sodium hydroxide, hydrochloric acid, fulvic acid (FA), potassium nitrate, potassium sulfate, potassium bicarbonate, isopropanol (IPA), sodium azide (NaN_3), and potassium sorbate (PS) were all analytical grade and purchased from Aladdin Reagent Co., Ltd. (Shanghai, China). MEF was dissolved in MilliQ-water to prepare a 100 mg L^{-1} stock solution and kept at $-20 \text{ }^\circ\text{C}$ before use. The concentration of the working solution was 0.5 mg L^{-1} .

Water sample

The effluent of a secondary sedimentation tank (ESST) was collected from a WWTP in Guangzhou City, China. TOC (TOC-V CPN, Shimadzu, Japan); main anions Cl^- , NO_3^- , SO_4^{2-} , and HCO_3^- (ion chromatography, ICS-1500, American Dion); conductivity (DDS-307, Shanghai Youyi Instrument Co., Ltd., Shanghai, China), and turbidity (WGZ-1B, Hangzhou Qiwei Instrument Co., Ltd., Hangzhou, China) were measured, and all characteristics are shown in Table S1 of the Supplementary Material.

Experimental methods

Photodegradation experiments

An UV-A-type high-pressure mercury lamp (125 W, 365 nm, Shanghai Jiguang, China) was selected as the light source in this study. The UV light spectrum of the lamp is shown in Fig. S1. A total of 100 mL of a 0.5-mg L^{-1} MEF solution was transferred to a cylindrical quartz reactor ($\phi 14 \text{ cm} \times 13 \text{ cm}$)

with a magnetic stirrer (85–2 Type, Shanghai Sile Equipment Co. Ltd., Shanghai, China) and the temperature of the system was controlled at 25 °C with circulating condensate. Before the light experiment, the high-pressure mercury lamp was turned on for 10 min to reach a steady state. The distance between the light source and liquid surface was 40 cm, and the optical power density 15.84 mW/cm² (CEL-NP2000, Beijing Zhongjiaojinyuan Technologies Co. Ltd., Beijing, China). The duration of light in the experiment was 360 min and a 1 mL sample was collected for analysis according to the method detailed in the “Chemical analysis method” section. Triplicates were conducted for each treatment and mean values were used to calculate the concentration and removal efficiencies. To deduce the influence of hydrolysis, a reactor with the same concentration of MEF was sealed with tin-foil paper and then placed under light conditions as a dark control.

Free radical quenching experiment

Studies have shown that isopropanol (IPA), sodium azide (NaN₃), and potassium sorbate (PS) can be used to quench hydroxyl radicals (·OH), ·OH and singlet oxygen (¹O₂), and triplet excited states (³ROM*) (Buxton et al. 1988; Chen et al. 2008; Miolo et al. 2002). These three radical quenchers were separately added to the UV photolysis reaction system at final concentrations of 2% IPA, 3 mM of NaN₃, and 3 mM of PS which can reduce the concentrations of ROS by 95% (Bodhipaksha et al. 2017). Other operations were the same as described in the “Photodegradation experiments” section.

Effect of pH, K⁺, NO₃⁻, Cl⁻, HCO₃⁻, and FA on the photolysis of MEF

To investigate the effects of the presence of different environmental factors on the photolysis of MEF, a series of single-factor experiments were conducted. A total of 0.2 M NaOH and 0.2 M HCl were used to adjust the working solution at pH 3, 5, and 7 with 0.1 M KH₂PO₄ and 0.1 M K₂HPO₄ as buffers to study the effect of pH value; NO₃⁻ (0, 0.6, 6, 31, and 62 mg L⁻¹), Cl⁻ (0, 0.4, 4, 18, and 36 mg L⁻¹), and HCO₃⁻ (0, 0.6, 6, 31, and 61 mg L⁻¹) were added separately to a 0.5 mg L⁻¹ MEF-phosphate buffer solution to test their effects on MEF photolysis. Then, 0, 1, 2, 5, and 30 mg L⁻¹ of FA (calculated by TOC; FA was extracted from lignite and its molecular weight was 308.24 g mol⁻¹) were added and the other operations were the same as in the “Photodegradation experiments” section. Since the buffers of all the solutions were prepared in potassium salt, K₂SO₄ was set as the control to deduce the effect of K⁺ and SO₄²⁻ on MEF photodegradation. The results show that both did not affect MEF photolysis (for the results, see Fig. S2).

Chemical analysis method

A 1.0 mL water sample was collected and passed through a 0.45 μm water-based filter membrane before analysis. MEF concentrations were determined by a high performance liquid chromatograph (HPLC, LC-20AT, Shimadzu, Japan) equipped with an UV detector and a ZORBAX Eclipse XDB-Phenyl column (5 μm, 4.6 × 150 mm). The mobile phase consisted of 0.01 M ammonium acetate (pH = 9) and acetonitrile in the ratio of 47.8:52.2 (v:v). The detection wavelength was 236 nm at a flow rate of 1 mL min⁻¹ at 40 °C with a column thermostat. The external standard method was used for calibration and the detection limit was three times of the standard deviation (10 μg L⁻¹).

Reaction kinetics calculations

The photodegradation of organic matter generally follows the characteristics of pseudo-first-order kinetics. The UV degradation of MEF and its half-life under UV light can be calculated by Eqs. (1) and (2), respectively:

$$\ln(C_t/C_0) = -kt \tag{1}$$

$$t_{1/2} = \ln 2/k \tag{2}$$

where C_t is the MEF concentration at time point t (mg L⁻¹); C₀ the initial concentration of (mg L⁻¹), k the pseudo-first-order kinetic reaction constant (min⁻¹), and t the reaction time (min).

Quantum yields of MEF were measured by a potassium ferric oxalate luminometer (Zepp 1978). When measuring the quantum yield of MEF, the MEF solution and the potassium ferric oxalate luminometer were placed under the same conditions for photolysis. The quantum yield of MEF can be calculated as

$$\varphi_A = \frac{k_B \sum L_\lambda \xi_\lambda^B}{k_A \sum L_\lambda \xi_\lambda^A} \varphi_B \tag{3}$$

where k_A is the reaction rate of the MEF (min⁻¹), k_B is the reaction rate of the potassium ferric oxalate (min⁻¹), ξ_λ is the molar absorption coefficient [L (mol cm⁻¹)⁻¹], L_λ is the relative light intensity, and φ_B is 1.24.

According to Eqs. (4)–(6) given in the literature (Lin et al. 2010), the contribution percentages of ·OH, ¹O₂, and ³ROM* to MEF photolysis can be estimated, respectively, as

$$R_{\cdot OH} = \frac{k - k_{IPA}}{k} \tag{4}$$

$$R_{^1 O_2} = \frac{k_{IPA} - k_{NaN_3}}{k} \tag{5}$$

$$R_{^3 ROM^*} = \frac{k - k_{PS}}{k} - R_{^1 O_2} \tag{6}$$

where R_{OH} , R_{1O_2} , and R_{3OM^*} are the contribution percentages of $\cdot OH$, 1O_2 , and $^3ROM^*$, respectively, to MEF photolysis; k_{IPA} , K_{NaN_3} , and k_{PS} are the photolysis rate constants when adding IPA, NaN_3 , and PS (min^{-1}), respectively.

The inhibition rate η of MEF photolysis by NO_3^- , Cl^- , HCO_3^- , and FA in the environment can be calculated by Eq. (7):

$$\eta = \frac{k - k_i}{k} \quad (7)$$

where k is MEF photolysis rate constant in working solution (min^{-1}) and k_i the photolysis rate constant in the presence of environmental factors such as NO_3^- , Cl^- , HCO_3^- , and FA (min^{-1}).

Nitrobenzene can be a molecular probe of $\cdot OH$ when reacting with organic compounds and the reaction rate of MEF with $\cdot OH$ can be obtained by Eq. (8) (Li 2016):

$$k_{OH} = \frac{\ln(C'_t/C'_0)}{\ln(S_t/S_0)} \times k_{OH}^s \quad (8)$$

where C'_t is the concentration of MEF at time point t (mg L^{-1}), C'_0 the initial concentration of MEF (mg L^{-1}), S_t the concentration of nitrobenzene at time point t (mg L^{-1}), S_0 the initial concentration of nitrobenzene (mg L^{-1}), and k_{OH}^s the rate constant when nitrobenzene and $\cdot OH$ react, $3.0 \times 10^9 \text{ L} \cdot (\text{mol s})^{-1}$.

According to Eq. (9), the reaction rate of MEF with 1O_2 can be obtained from the competitive kinetics of 1O_2 with MEF and furfuryl alcohol (FFA) (Haag and Hoigne 1986):

$$k_{1O_2} = \frac{\ln(S'_t/S'_0)}{\ln(R_t/R_0)} \times k_{1O_2}^R \quad (9)$$

where S'_t is the concentration of MEF at time point t (mg L^{-1}), S'_0 initial concentration of MEF (mg L^{-1}), R_t the concentration of FFA at time point t (mg L^{-1}), R_0 the original concentration of FFA (mg L^{-1}), and $k_{1O_2}^R$ the reaction rate constant of FFA and 1O_2 , $1.2 \times 10^8 \text{ L} \cdot (\text{mol s})^{-1}$.

Light screening effect calculation

The light screening effect coefficients of environmental factors can be calculated by Eqs. (10) and (11). The smaller the overall light screening coefficient, the stronger the light screening effect.

$$S_\lambda = \frac{1 - (10^{-(\alpha_\lambda + \xi_\lambda [MEF]l)})}{2.303(\alpha_\lambda + \xi_\lambda [MEF]l)} \quad (10)$$

$$\sum_{200 \leq \lambda \leq 400} S_\lambda = \frac{\sum L_\lambda \xi_\lambda S_\lambda}{\sum L_\lambda S_\lambda} \quad (11)$$

where S_λ is the light screening coefficient of a certain ion for MEF at a certain wavelength, α_λ the extinction coefficient of a certain concentration of the environmental factors (cm^{-1}), ξ_λ the molar absorption coefficient ($\text{L} \cdot (\text{mol cm})^{-1}$), $[MEF]$ the concentration of MEF (mol L^{-1}), l the light distance (cm), L_λ the relative light intensity, and $\sum S_\lambda$ the overall light screening coefficient.

The photolysis rates and the light screening effect when environmental factors (NO_3^- , Cl^- , HCO_3^- , FA) are presented can be calculated by Eqs. (12) and (13).

$$k'_i = \sum S_\lambda k \quad (12)$$

$$\eta' = \frac{k'_i - k}{k} \quad (13)$$

where k'_i is the light screening reaction rate constant of MEF when an environmental factor is present (min^{-1}), $\sum S_\lambda$ is the light screening coefficient, k is MEF photolysis rate constant in the working solution (min^{-1}) (without the substance with light screening effect), and η' is the inhibition rate of the light screening effect.

DFT computational methods

The DFT calculations involved were all performed in the GAUSSIAN 09 software package (Frisch et al. 2009) and the DFT method used in this study is the M06-2x method (Zhao and Truhlar 2008). The geometrical parameters of MEF and its products contained in the reaction were optimized at the M06-2x/6-311 + G(d, p) level. To obtain the total electron energies accurately, single-point energies were calculated at the more precise level of M06-2x/6-311 + G(d, p) level, i.e., at the M06-2x/6-311++G(2d, p) level. The zero point energy (ZPE) corrections were included for all energies (Table S2) (Alecu et al. 2010). In this study, a solvation model based on density (SMD), i.e., a continuum solvent model, was used to consider the solvent effect in all work (Marenich et al. 2009).

Identification of photolysis intermediates

The photolysis intermediates were identified by UPLC1290-6540B Q-TOF (Agilent, USA; AB SCIEX™, USA) equipped with an HILIC plus C18 instrument (1.8 μm , $2.1 \times 100 \text{ mm}$). The mobile phase consisted of acetonitrile and MilliQ water (with 0.2% formic acid and 5 mM ammonium formate) with an injection volume of 100 μL at 40 °C with a column thermostat (Martin et al. 2012). The gradient elution conditions are shown in Table S3. The analysis was performed in positive and negative ion modes (ESI \pm) with a Triple TOF™ 6540B device (AB SCIEX™, USA), the data acquisition range was 50–1000 m/z, and the collection interval was 0.1 s. The specific parameter settings are listed in Table S4.

Results and discussion

Photolysis kinetics of MEF

A 25-day dark control showed that MEF experienced no obvious reduction (< 2%) and that the effect of natural hydrolysis could be neglected during photolysis. Figure 1 shows the MEF degradation in the prepared working solution and ESST when UV irradiation was conducted and both followed the pseudo-first-order kinetic model. After photodegradation for 360 min, the degradation rate constant in pure water was 0.0029 min⁻¹, which was slower than that of MEF in the ESST (0.0090 min⁻¹). The promotion of MEF photodegradation may be due to the active species, e.g., ROS generated by chemical reactions in the sewage. This result also indicates that the degradation of MEF occurs mainly through indirect photodegradation. Studies have shown that nitrate and humus in sewage are photosensitizers that can produce active substances that affect the photolysis behavior of target compounds (Ryan et al. 2011). Comparing the reactions in pure water and an ESST, it is speculated that the composition of water has an important influence on the photolysis of MEF. To clarify their role in promoting or inhibiting the photolysis of MEF, the effects of different environmental factors on the photolysis of MEF in saline solution was investigated (see the “Factors affecting photodegradation of MEF” section).

Mechanisms of MEF degradation under UV

In a water body, the direct photolysis reaction and indirect self-sensitive photolysis processes of organic matter are common. Quenchers were added into the ESST to test the generation of ROS in the MEF photolysis process, and the results are shown in Fig. 2 (for kinetics parameters, see Table S5).

It can be concluded that the photolysis of MEF was inhibited when quenchers were added. The inhibition sequence is NaN₃ > IPA > PS and the contribution percentages of for ·OH, ³ROM*, and ¹O₂ are 73%, 11%, and 8%,

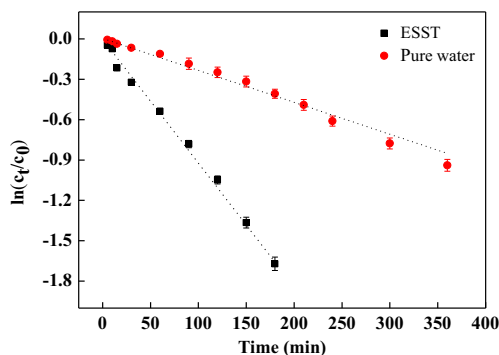


Fig. 1 Degradation kinetics of MEF in pure water and ESST (pH = 7, 25 °C)

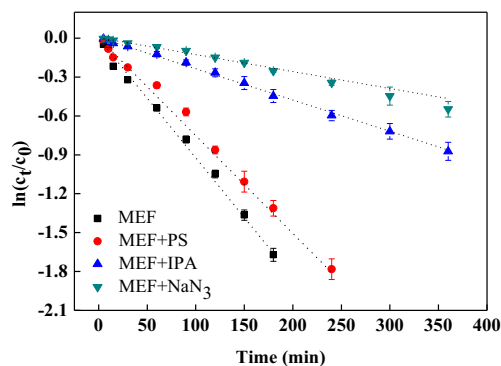


Fig. 2 Effects of different quenchers on photolysis of MEF in ESST (pH = 7, 25 °C)

respectively, in the ESST, which demonstrates that all three ROS were involved in the photolysis of MEF and that ·OH may play a major role. The direct photolysis was only 7% or so during the photodegradation process. In summary, it can be inferred that the photolysis mechanism of MEF is that (1) MEF is converted into active ³MEF* by photoabsorption of photons and then direct photolysis occurs; (2) ³MEF* transfers energy to dissolved oxygen (DO) in solution to generate ROS, which oxidatively degrade MEF; and (3) DOM generates ROS by chemical reaction and then oxidatively degrades MEF.

It has been reported that a variety of ROS can be formed in the surface water under sunlight, and the concentration of ·OH is in the range of approximately 10⁻¹⁷–10⁻¹⁵ (mol L⁻¹). In the natural environment, the concentration of ·OH in water depends on the water’s composition (Cooper et al. 2009). From the ·OH oxidation of MEF competition kinetics curve (Fig. S2), the reaction rate of MEF and ·OH is (6.45 ± 0.40) × 10⁹ L·(mol s)⁻¹ in ESST. ¹O₂ is an important type of electrophilic ROS in natural water, which is an unstable singlet oxygen molecule in an excited state (10⁻⁶–10⁻⁵ s) (Zepp et al. 1977). The photodegradation kinetics of MEF and FFA are shown in Fig. S3, and the calculation of the competition kinetic equation shows that the reaction rate of MEF and ¹O₂ was determined to be (5.4 ± 0.7) × 10⁶ L·(mol s)⁻¹ in the ESST, because the existence time of ¹O₂ is very short and its reaction rate of MEF is much slower than that of ·OH, which also indicates that ·OH plays a major role in MEF photolysis.

Factors affecting photodegradation of MEF

pH value

MEF has two different pK_a values, corresponding to pK₁ = 2.8 and pK₂ = 11.6, which results in MEF having both molecular and ionic states. Since the high pH lowered the detection accuracy of the instrument, the degradation of MEF under acidic and neutral conditions was carried out in this study and the results are shown in Fig. 3. It can be seen that the

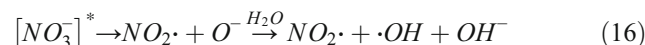
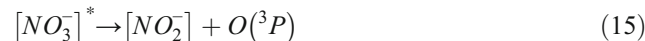
degradation rate constant of MEF increased from 0.0015 to 0.0031 min⁻¹ when the pH increased from 3 to 7, and the inhibition rates decreased from 52 to 0% (see Table S6). Under acidic conditions, the photodegradation rate of MEF was slower than that under neutral conditions. This is because the main form of MEF is C₄H₁₁N₅ when the pH is lower than 3, C₄H₁₂N₅⁺ when 3 < pH < 11, and C₄H₁₃N₅²⁺ when pH > 11 (Zhu et al. 2017). As the pH increases, molecular MEF decreases and ionic MEF increases. Such state change is beneficial to the attack of strong electrophilic ·OH, leading to an accelerated photolysis rate of MEF. Moreover, the base catalysis may occur so that the yield of ·OH increases with increasing pH (Lam et al. 2005; Latch et al. 2003), which promotes the photolysis of MEF.

Nitrate

NO₃⁻ is one of the most common anions in many water bodies, and the previous study reported the promotion and inhibition effects on the photolysis of organic pollutants (OPs) (Wang et al. 2017). Jacobs et al. reported that NO₃⁻ promotes photolysis of caffeine in water (Jacobs et al. 2012). However, Wang et al. found that for 2,4-D, simazine and diuron, low concentrations (10 mg L⁻¹) of NO₃⁻ promoted the photolysis of pollutants, while high concentrations (20 mg L⁻¹) of NO₃⁻ inhibited degradation of pollutants. To investigate the role of NO₃⁻ in MEF photolysis, 0.6–60 mg L⁻¹ NO₃⁻ (from KNO₃) was added to the solution, and the results are shown in Fig. 4a. It can be seen that the photodegradation of MEF still conforms to the pseudo-first-order reaction kinetics equation and that the photodegradation rate of MEF has a positive correlation with NO₃⁻ concentration (kinetics parameters are listed in Table 1).

The effect of NO₃⁻ could be interpreted as a competitive relationship between inhibition and promotion; that is, between the light screening effect and ·OH generation. On one hand, NO₃⁻ can promote the production of ·OH, which is the dominant ROS in this study. The ·OH formation process could be expressed as Eqs. (14)–(16) (Wang et al. 2017). On the other hand, NO₃⁻ can compete with the chemical to absorb

photons (the quantum yield of MEF is 0.7) and inhibit the photodegradation of MEF:



It can be found from Table 1 that the light screening effect coefficients range from 0.0026 to 0.0015, which inhibited the photolysis, i.e., from 17.1 to 51.7%. However, the negative value of η means the promotion of MEF photolysis. Comparing with η and η' , it can be concluded that the effect of excited ROS (its contribution is represented by $\eta-\eta'$) is greater than that of the light screening effect, which shows the overall promotion of MEF photolysis.

Cl⁻

Cl⁻ is the main anion component in water, and its effect on the photolysis of pollutants is not negligible. The overall effect of Cl⁻ on the photodegradation of MEF changed from promotion to inhibition for increasing chloride concentrations (Fig. 4b and Table 1). The effect of Cl⁻ on MEF photolysis was a combination of the following three factors,

- 1) The light screening effect, which ranged from 16.0 to 25.4% when the concentration of Cl⁻ was increased from 0.4 to 36 mg L⁻¹. The insignificant increase in the case of a 90-fold increase in concentration implied that the light screening effect may not be the dominant factor for MEF photolysis.
- 2) ROS quenching, i.e., Cl⁻ can quench a small part of the ·OH in the aqueous solution to form ·Cl; the reaction rate of Cl⁻ with ·OH was 1 × 10⁹ L·(mol s)⁻¹ (Buxton et al. 1988).
- 3) Photolysis promotion, i.e., Cl⁻ can induce the production of reactive halogen species (RHS, e.g., X· and X₂⁻) and ¹O₂. These RHSs, residual ·OH, and ¹O₂ can promote the photolysis of MEF.

In this study, when lower concentrations of Cl⁻ (< 4 mg L⁻¹) were added, the co-existence of ·Cl and ·OH could promote the photolysis of MEF although Cl⁻ quenched part of ·OH in the solution. When the concentration of Cl⁻ increased, it quenched a large amount of ·OH and triplet DOM (Chiron et al. 2006), leading to the overall inhibition of MEF photolysis.

HCO₃⁻

Bicarbonate is a photosensitive substance commonly found in natural waters, and its presence may also interfere with the

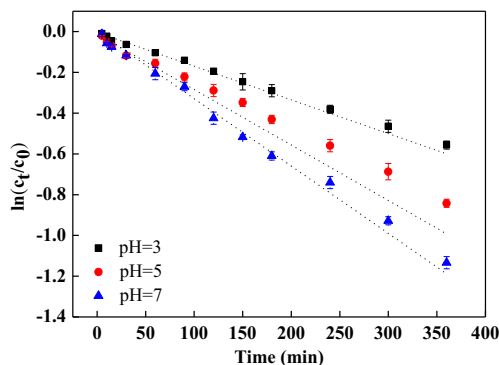
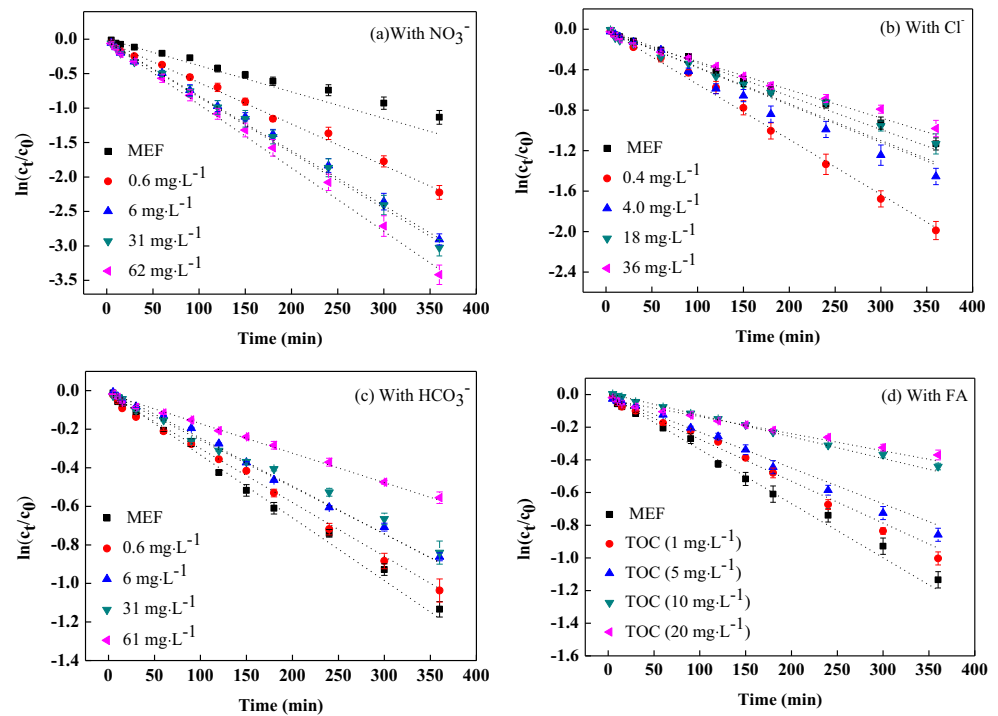


Fig. 3 Photodegradation of MEF under different pH conditions

Fig. 4 Photodegradation kinetic curves of different influencing factors coexisting with MEF



photodegradation behavior of MEF. The effect of HCO_3^- on MEF photolysis is shown in Fig. 4c. After adding HCO_3^- , the photodegradation rate of MEF decreased with increasing HCO_3^- concentration in the solution. Since HCO_3^- is a scavenger of $\cdot\text{OH}$, and its reaction rate with $\cdot\text{OH}$ is $8.15 \times 10^6 \text{ L} \cdot (\text{mol s})^{-1}$ (Eq. (17)), there is also a slight light screening effect for HCO_3^- (Buxton et al. 1988; Tercero et al. 2007). The inhibition rate increased from 9.7 to 51.6% when the

concentrations of HCO_3^- increased from 0.6 to 64 mg L^{-1} (data are shown in Table 1). Comparing η - η' values of HCO_3^- addition, it can be concluded that the quenching effect is greater than that of the light screening effect:

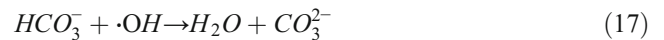
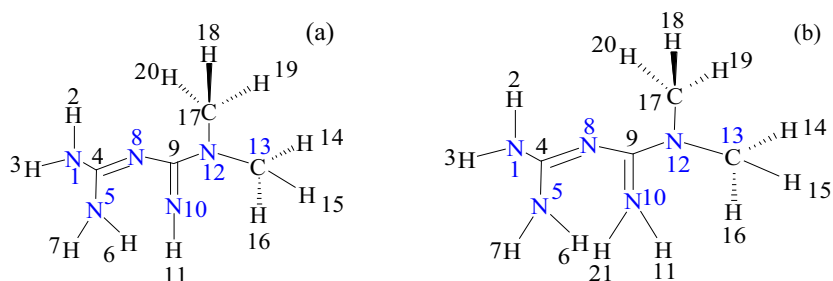


Table 1 Photodegradation rate constants, half-lives, and inhibition rates of metformin (MEF) coexisting with different influencing substances

	Concentration/ mg L^{-1}	$t_{1/2}/\text{min}$	η	k'/min^{-1}	η'	$\eta-\eta'$
MEF	0.50	238.9	/	/	/	/
with NO_3^-	0.6	117.5	-90.3%	0.0026	17.1%	-107.4%
	6	90.2	-148.4%	0.0023	25.3%	-173.6%
	31	86.6	-158.1%	0.0017	46.3%	-204.4%
	62	77.2	-193.5%	0.0015	51.7%	-245.2%
with Cl^-	0.4	123.8	-80.6%	0.0026	16.0%	-96.6%
	4	169.1	-32.3%	0.0026	17.7%	-49.9%
	18	231.0	3.2%	0.0025	20.6%	-17.4%
	36	266.6	16.1%	0.0023	25.4%	-9.3%
with HCO_3^-	0.6	247.6	9.7%	0.0028	8.6%	1.1%
	6	288.8	22.6%	0.0027	11.7%	10.9%
	31	315.1	29.0%	0.0026	15.7%	13.3%
	61	462.1	51.6%	0.0025	19.4%	32.2%
with FA	1	239.0	12.9%	0.0027	13.4%	-0.5%
	5	288.8	22.6%	0.0022	28.7%	-6.1%
	10	577.6	61.3%	0.0016	47.7%	13.6%
	20	770.1	71.0%	0.0014	53.2%	17.7%

Fig. 5 Atomic ordering of MEF in **a** molecular and **b** cationic forms during DFT computation



FA

DOM is a ubiquitous matrix that produces ROS such as triplet excited-state organics ($^3\text{OM}^*$), singlet oxygen ($^1\text{O}_2$), and hydroxyl radicals ($\cdot\text{OH}$) (He et al. 2018). The largest component of DOM in surface water and sewage matrix is humus, of which humic acid and fulvic acid are the main components. Similar to NO_3^- , humus has promotion and inhibition effects on the photolysis of OPs. From the aspect of promotion, it has been reported that humus can transfer energy to OPs or to dissolved oxygen (DO) to form ROS ($\cdot\text{OH}$, $^1\text{O}_2$, or other active oxidation intermediates), causing OP degradation (Makunina et al. 2015; Pozdnyakov et al. 2017). As for inhibition, the UV wavelength range of humus (190–400 nm) overlaps that of many OPs, which can compete as a light source with pollutants. Consequently, OPs masks photons or quenches active oxides, causing photodegradation to be suppressed (Zeng et al. 2012; Zepp et al. 1985). It can be seen from Fig. 4d and Table 1 that the addition of FA significantly reduced the photolysis rate of MEF, and its overall inhibition increased from 12.9 to 71.0% (Table 1). Comparing η - η' values of FA addition, it can be concluded that the light screening effect is dominant in MEF photolysis.

DFT computation and photolysis product identification by UPLC/Q-TOF-MS

Frontier orbital theory was used to calculate the cleavage position of MEF by oxidative degradation, and the UV oxidation products of MEF were detected with UPLC/Q-TOF-MS to verify the theoretical analysis results. According to the frontier orbital theory of Fukui (Fukui et al. 1954), the calculation of the frontier electron density f_r is expressed by Eq. (18):

$$f_r = \sum_i (C_{ri}^{\text{HOMO}})^2 + \sum_i (C_{ri}^{\text{LUMO}})^2 \quad (18)$$

where r is the number of carbon, nitrogen, or hydrogen atoms in i : 2 s, 2p_x, 2p_y, and 2p_z orbitals. C_{ri}^{HOMO} and C_{ri}^{LUMO} are the orbital coefficients of each orbit of each atom in the highest occupied molecular orbital (HOMO) and lowest unoccupied molecular orbital (LUMO). The values of $[(C_{ri}^{\text{HOMO}})^2 + (C_{ri}^{\text{LUMO}})^2]$ were calculated from Gaussian output files to predict the feasible sites for $\cdot\text{OH}$ attack (Fukui et al. 1952; Fukui et al. 1954). The highest f_r value indicates the most reactive position, i.e., that most likely to be attacked by a radical.

Table 2 Frontier electron densities of molecular and cationic forms of MEF (M06-2x/6-31 + G(d, p)/SMD)

Atoms	Frontier electron densities		Atoms	Frontier electron densities	
	C ₄ H ₁₁ N ₅	C ₄ H ₁₂ N ₅ ⁺		C ₄ H ₁₁ N ₅	C ₄ H ₁₂ N ₅ ⁺
1(N)	0.02407	0.14422	12(N)	0.42429	0.41882
2(H)	0.01302	0.00665	13(C)	0.01033	0.02562
3(H)	0.02291	0.00860	14(H)	0.01196	0.01277
4(C)	0.00502	0.18866	15(H)	0.03007	0.03417
5(N)	0.00836	0.09899	16(H)	0.00320	0.01058
6(H)	0.00282	0.01244	17(C)	0.01930	0.02540
7(H)	0.01366	0.00543	18(H)	0.04022	0.02690
8(N)	0.01325	0.36319	19(H)	0.01628	0.01957
9(C)	0.00847	0.23244	20(H)	0.00338	0.00126
10(N)	0.40952	0.08841	21(H)	/	0.00540
11(H)	0.00148	0.01381	Value summation	1.08168	1.74339

Table 3 Possible intermediate information of MEF under UV irradiation

Intermediates	Retention time (min)	<i>m/z</i>	Predicted molecular formula	Error (ppm)
P1	1.595	126.1	C ₄ H ₇ N ₅	1.74
P2	1.765	112.1	C ₃ H ₆ N ₅	0.78
P3	4.763	127.1	C ₃ H ₉ N ₃	3.79
P4	4.781	88.1	C ₄ H ₇ N ₅	-2.62
P5	4.847	116.1	C ₃ H ₉ N ₅	1.17
P6	4.963	102.1	C ₂ H ₇ N ₅	-0.77

According to Eq. (12), frontier electron densities of all C, N, and H atoms in molecular and cationic MEF (atomic ordering is shown in Fig. 5) were calculated and are given in Tables 2 and S7.

Frontier orbital theory shows that an atom with higher frontier electron density is more susceptible to being attacked by ·OH. As can be seen in Table 2, N12 and N10 atoms had the highest frontier electron densities, 0.42429 and 0.40952, respectively, in molecular form MEF. Thus, it was suggested that N12 and N10 atoms would be the primary sites attacked by ·OH; the order of being attacked is N12 > N10. In the cationic form of MEF, N12 and N8 atoms have higher front electron densities, 0.41882 and 0.36319, respectively (Table 2). N12 and N8 atoms are the main sites of ·OH attack. There are many sites on the MEF parent compound that can react with ·OH, such as C=N bonds (at position C9) and H atoms on two methyl groups (at positions H14, H15, H16, H18, H19, and H20). However, the front electron density of H atoms on MEF is low, and the hydrogen extraction reaction occurs with greater difficulty.

To verify the theoretical calculations, we identified the products after photolysis of MEF using UPLC/Q-TOF. Under UV irradiation, in addition to the MEF (detected at

RT = 4.785 min), there are six photolysis products at RT from 1.633 to 5.049 min (Table 3), and their secondary mass spectra are shown in Fig. S5.

When attacked by ·OH, the C-N bond at the N12 site was broken to lose -CH₃ to form demethylated MEF and was consequently protonated to form P5, methyl metformin (MBG, Fig. 6, pathway A), for which *m/z* = 116.1. MBG can continue to form an excited MBG, which may undergo cyclization to form P2—that is, 2,4-diamino-1,3,5-triazine (2,4-DAT, Fig. 6, pathway A-1) at *m/z* = 112.1—and may continue to demethylate to form P6, biguanide (BGN, Fig. 6, pathway A-2) at *m/z* = 102.1. The ion detected at *m/z* = 88.1 may be P4; that is, 1,1-dimethylhydrazine (1,1-DiMBG, Fig. 6, pathway B) formed when C=N was attacked at N8. The formation of P1, which is called 4-amino-2-imino-1-methyl-1,2-dihydro-1,3,5-triazine (4,2,1-AIMT, Fig. 6, pathway C), detected at *m/z* = 126.1, was obtained through the di-dehydrogenation of MEF. P3 at *m/z* = 127.1 may be 2-amino-4-methylamino-1,3,5-triazine (2,4-AMT, Fig. 6, pathway C), i.e., the rearranged product of 4,2,1-AIMT. Therefore, the possible pathway for oxidative degradation of MEF under UV irradiation is proposed as depicted in Fig. 6.

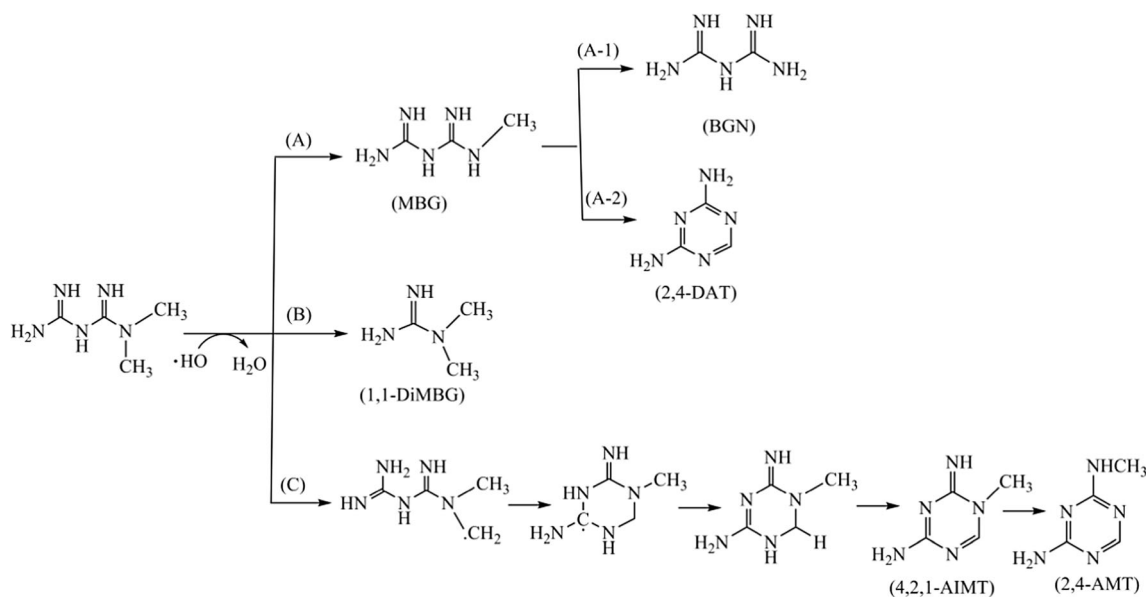


Fig. 6 Possible oxidative degradation pathway of MEF under UV irradiation

For organic pollutants, the site of free radical attack and the position of easily broken bonds can be predicted by analyzing the size of the bond dissociation energy (BDE). The higher the BDE, the more difficult it is to break the chemical bond. Whether the reaction is easy or not was judged by the corresponding BDE in the A, B, C, A-1, and A-2 pathways of MEF photolysis as shown in Fig. 6. The N12-C17 bond has the lowest BDE (78.7 kcal mol⁻¹), followed by 92.3 kcal mol⁻¹ for C13-H16 and 97.0 kcal mol⁻¹ for the N8-N4 bond. Thus, the order from easy to difficult for the photolysis reaction is A > C > B. For the A-1 and A-2 pathways, the BDE of the N12-C17 bond is 88.4 kcal mol⁻¹ and that of C17-H18 is 93.2 kcal mol⁻¹; therefore, the A-1 reaction path is more likely to occur than that of A-2. It is also demonstrated that N12 is the most vulnerable to ·OH attack sites, which is consistent with the calculation results of the frontier electron density. When MEF exists in a cationic form, N8 is also a susceptible site to ·OH attack, which will induce the B reaction pathway to occur.

Conclusions

In this study, the photodegradation mechanism and kinetic model of MEF photolysis under UV light irradiation were studied. The effects of pH value, various coexisting substances (nitrate, fulvic acid, chloride, bicarbonate, etc.), and the related mechanisms were investigated as well. The results showed the following.

- (1) Self-sensitized photolysis is the primary process that conforms to the pseudo-first-order kinetic model.
- (2) The ·OH radical plays a major role in the photolysis of MEF.
- (3) NO₃⁻ is the main source of the ·OH that can accelerate the photolysis reaction rate.
- (4) The effect of the light screening effect of FA is greater than the promotion of ·OH generation, causing the inhibition of MEF photolysis.
- (5) Cl⁻ and HCO₃⁻ had inhibitory effects on MEF photolysis because of the quenching of ·OH.
- (6) The UV-oxidized products identified by UPLC/Q-TOF were consistent with the results of DFT calculations and their pathways proposed.

Acknowledgments We would like to thank Dr. Pu Ge for the help on DFT calculation, Dr. Fuhua Li for the calculation of light screening effect and quantum yield, and LetPub (www.letpub.com) for its linguistic assistance during the revision of this manuscript.

Funding information This work was supported by the National Natural Science Foundation of China (Grant No. 41877466), Natural Science Foundation of Guangdong Province (Grant No. 2019A1515011037), Research Fund of SIT of Guangzhou (Grant No. 201707010158).

Compliance with ethical standards

Ethics statement This paper is our original work. Authorship of the paper included all those who have made significant contributions to the work and they are listed as co-authors. All co-authors have approved the final version of the paper and have agreed to its submission for publication. We have not already published in another journal a paper describing essentially the same material, nor is this paper currently being considered for publication in another journal. All sources of financial support had been disclosed in the Acknowledgments. All authors accepted these principles as mentioned above.

Conflict of interest The authors declare that they have no conflict of interest.

References

- Alecu IM, Zheng J, Zhao Y, Truhlar DG (2010) Computational thermochemistry: scale factor databases and scale factors for vibrational frequencies obtained from electronic model chemistries. *J Chem Theory Comput* 6(9):2872–2887
- Blair B, Nikolaus A, Hedman C, Klaper R, Grundl T (2015) Evaluating the degradation, sorption, and negative mass balances of pharmaceuticals and personal care products during wastewater treatment. *Chemosphere* 134:395–401
- Bodhipaksha LC, Sharpless CM, Chin Y, MacKay AA (2017) Role of effluent organic matter in the photochemical degradation of compounds of wastewater origin. *Water Res* 110:170–179
- Buxton GV, Greenstock CL, Helman WP, Ross AB (1988) Critical review of rate constants for reactions of hydrated electrons, hydrogen atoms and hydroxyl radicals (·OH/·O⁻) in aqueous solution. *J Phys Chem Ref Data* 17(2):513–886
- Campbell A J. 2013. The behaviour of pharmaceuticals in anaerobic digester sludge. University of Portsmouth
- Chen Y, Hu C, Qu J, Yang M (2008) Photodegradation of tetracycline and formation of reactive oxygen species in aqueous tetracycline solution under simulated sunlight irradiation. *J Photoch Photobio A* 197(1):81–87
- Cheng S, Zhang X, Yang X, Shang C, Song W, Fang J, Pan Y (2018) The multiple role of bromide ion in PPCPs degradation under UV/chlorine treatment. *Environ Sci Technol* 52(4):1806–1816
- China Industry Information Network (2018) 2017 China's diabetes industry development trend and market size forecast, <http://www.chyxx.com/industry/201701/485956.html>. Accessed 22 Dec 2018
- Chiron S, Minero C, Vione D (2006) Photodegradation processes of the antiepileptic drug carbamazepine, relevant to estuarine waters. *Environ Sci Technol* 40(19):5977–5983
- Collin F, Khoury H, Bonnefont-Rousselot D, Théron P, Legrand A, Jore D, Gardès-Albert M (2004) Liquid chromatographic/electrospray ionization mass spectrometric identification of the oxidation end-products of metformin in aqueous solutions. *J Mass Spectrom* 39(8):890–902
- Cooper WJ, Zika RG, Petasne RG, Fischer AM (2009) Sunlight-induced photochemistry of humic substances in natural-waters - major reactive species. *Adv Chem* 219(1):333–362
- Crago J, Bui C, Grewal S, Schlenk D (2016) Age-dependent effects in fathead minnows from the anti-diabetic drug metformin. *Gen Comp Endocrinol* 232:185–190
- Editorial Department Of Annual Report (2017) Chemical pharmaceuticals division in 2015 China medical statistics annual report. Ministry of Industry and Information Technology of China, Beijing, p 157

- Editorial Department Of Annual Report (2018) Chemical pharmaceuticals division in 2016 China medical statistics annual report. Ministry of Industry and Information Technology of China, Beijing, p 153
- Escher BI, Rebekka B, Mirjam K, Karin T, Judit L, Mcardell CS (2011) Environmental toxicology and risk assessment of pharmaceuticals from hospital wastewater. *Water Res* 45(1):75–92
- Frisch M J, Trucks G W, Schlegel H B, Scuseria G E, Robb M A, Cheeseman J R. (2009). *Gaussian 09, Revision a.02*. Gaussian, Inc., Wallingford, CT, USA
- Fukui K, Yonezawa T, Shingu H (1952) A molecular orbital theory of reactivity in aromatic hydrocarbons. *J Chem Phys* 20:722–725
- Fukui K, Yonezawa T, Nagata C, Shingu H (1954) Molecular orbital theory of orientation in aromatic, heteroaromatic, and other conjugated molecules. *J Chem Phys* 22(8):1433–1442
- Haag WR, Hoigne J (1986) Singlet oxygen in surface waters. 3. Photochemical formation and steady-state concentrations in various types of waters. *Environ Sci Technol* 20(4):341–348
- He H, Xiong D, Han F, Xu Z, Huang B, Pan X (2018) Dissolved oxygen inhibits the promotion of chlorothalonil photodegradation mediated by humic acid. *J Photoch Photobio A* 360:289–297
- Jacobs LE, Weavers LK, Houtz EF, Chin YP (2012) Photosensitized degradation of caffeine: role of fulvic acids and nitrate. *Chemosphere* 86(2):124–129
- Lam MW, Young CJ, Mabury SA (2005) Aqueous photochemical reaction kinetics and transformations of fluoxetine. *Environ Sci Technol* 39(2):513–522
- Latch DE, Packer JL, Arnold WA, McNeill K (2003) Photochemical conversion of triclosan to 2,8-dichlorodibenzo-p-dioxin in aqueous solution. *J Photoch Photobio A* 158(1):63–66
- Li F (2016) Study on photolytic behavior and mechanisms of ibuprofen in aqueous environment. Guangdong University of Technology, Guangzhou, p 163
- Li Y, Pan Y, Lian L, Yan S, Song W, Yang X (2017) Photosensitized degradation of acetaminophen in natural organic matter solutions: the role of triplet states and oxygen. *Water Res* 109:266–273
- Lin K, Chen J, Zhang S, Xi Y, Wang Z, Wang C (2010) Photodegradation of fluoroquinolone antibiotic gatifloxacin in aqueous solutions. *Chin Sci Bull* 55(15):1495–1500
- Ma J, Lv W, Chen P, Lu Y, Wang F, Li F, Yao K, Liu G (2016) Photodegradation of gemfibrozil in aqueous solution under UV irradiation: kinetics, mechanism, toxicity, and degradation pathways. *Environ Sci Pollut Res Int* 23(14):14294–14306
- Makunina MP, Pozdnyakov IP, Chen Y, Grivin VP, Bazhin NM, Plyusnin VF (2015) Mechanistic study of fulvic acid assisted propranolol photodegradation in aqueous solution. *Chemosphere* 119:1406–1410
- Marenich AV, Cramer CJ, Truhlar DG (2009) Universal solvation model based on solute electron density and on a continuum model of the solvent defined by the bulk dielectric constant and atomic surface tensions. *J Phys Chem B* 113(18):6378–6396
- Martin J, Buchberger W, Luis Santos J, Alonso E, Aparicio I (2012) High-performance liquid chromatography quadrupole time-of-flight mass spectrometry method for the analysis of antidiabetic drugs in aqueous environmental samples. *J Chromatogr B* 895:94–101
- Miolo G, Viola G, Vedaldi D, Dall'Acqua F, Fravolini A, Tabarrini O, Cecchetti V (2002) In vitro phototoxic properties of new 6-desfluoro and 6-fluoro-8-methylquinolones. *Toxicol in Vitro* 16(6):683–693
- Niemuth NJ, Klaper RD (2015) Emerging wastewater contaminant metformin causes intersex and reduced fecundity in fish. *Chemosphere* 135:38–45
- Ogurtsova K, Da RFJ, Huang Y, Linnenkamp U, Guariguata L, Cho NH, Cavan D, Shaw JE, Makaroff LE (2017) IDF diabetes atlas: global estimates for the prevalence of diabetes for 2015 and 2040. *Diabetes Res Clin Pract* 128:40–50
- Pozdnyakov IP, Salomatova VA, Parkhats MV, Dzharagov BM, Bazhin NM (2017) Efficiency of singlet oxygen generation by fulvic acids and its influence on UV photodegradation of herbicide Amitrole in aqueous solutions. *Mendeleev Commun* 27(4):399–401
- Quintao FJO, Freitas JRL, Machado CDF, Aquino SF, Silva SDQ, Afonso RJDC (2016) Characterization of metformin by-products under photolysis, photocatalysis, ozonation and chlorination by high-performance liquid chromatography coupled to high-resolution mass spectrometry. *Rapid Commun Mass Spectrom* 30(21):2360–2368
- Ryan CC, Tan DT, Arnold WA (2011) Direct and indirect photolysis of sulfamethoxazole and trimethoprim in wastewater treatment plant effluent. *Water Res* 45(3):1280–1286
- Scheurer M, Sacher F, Brauch H (2009) Occurrence of the antidiabetic drug metformin in sewage and surface waters in Germany. *J Environ Monit* 11(9):1608–1613
- Scheurer M, Michel A, Brauch HJ, Ruck W, Sacher F (2012) Occurrence and fate of the antidiabetic drug metformin and its metabolite guanilurea in the environment and during drinking water treatment. *Water Res* 46(15):4790–4802
- Tang T, Lord JM, Norman RJ, Yasmin E, Balen AH (2012) Insulin-sensitising drugs (metformin, rosiglitazone, pioglitazone, D-chiro-inositol) for women with polycystic ovary syndrome, oligo amenorrhoea and subfertility. *Cochrane Db Syst Rev* 84(1):CD003053
- Tercero ELA, Neamtu M, Frimmel FH (2007) The effect of nitrate, Fe(III) and bicarbonate on the degradation of bisphenol a by simulated solar UV-irradiation. *Water Res* 41(19):4479–4487
- Tisler S, Zwiener C (2019) Aerobic and anaerobic formation and biodegradation of guanil urea and other transformation products of metformin. *Water Res* 149:130–135
- Trautwein C, Kümmerer K (2011) Incomplete aerobic degradation of the antidiabetic drug metformin and identification of the bacterial dead-end transformation product guanilurea. *Chemosphere* 85(5):765–773
- Wang Y, Roddick FA, Fan L (2017) Direct and indirect photolysis of seven micropollutants in secondary effluent from a wastewater lagoon. *Chemosphere* 185:297–308
- Yong C, Hu C, Hu XX, Qu JH (2009) Indirect photodegradation of amine drugs in aqueous solution under simulated sunlight. *Environ Sci Technol* 43(8):2760–2765
- Zeng C, Ji Y, Zhou L, Zhang Y, Yang X (2012) The role of dissolved organic matters in the aquatic photodegradation of atenolol. *J Hazard Mater* 239-240:340–347
- Zepp RG (1978) Quantum yields for reaction of pollutants in dilute aqueous solution. *Environ Sci Technol* 12(3):327–329
- Zepp RG, Wolfe NL, Baughman GL, Hollis RC (1977) Singlet oxygen in natural waters. *Nature* 266(5600):421–423
- Zepp RG, Schlotzhauer PF, Sink RM (1985) Photosensitized transformations involving electronic energy transfer in natural waters: role of humic substances. *Environ Sci Technol* 19(1):74–81
- Zhao Y, Truhlar DG (2008) The M06 suite of density functionals for main group thermochemistry, thermochemical kinetics, noncovalent interactions, excited states, and transition elements: two new functionals and systematic testing of four M06-class functionals and 12 other functionals. *Theor Chem Accounts* 120(1–3):215–241
- Zhu S, Liu YG, Liu SB, Zeng GM, Jiang LH, Tan XF, Zhou L, Zeng W, Li TT, Yang CP (2017) Adsorption of emerging contaminant metformin using graphene oxide. *Chemosphere* 179:20–28